Biochemistry and Biophysics Reports 40 (2024) 101833

Contents lists available at ScienceDirect

Biochemistry and Biophysics Reports

journal homepage: www.elsevier.com/locate/bbrep

CEACAM1 increased the lymphangiogenesis through miR-423-5p and NF-kB in Non-Small Cell Lung Cancer

Jie Yu [a,1], Wenke Cai [a,1], Tao Zhou [b], Bo Men [a], Shunqiong Chen [b], Dong Tu [a], Wei Guo [a], Jicui Wang [a], Feipeng Zhao [c,*], Yan Wang [d,**]

[a] Department of Thoracocardiac Surgery, 920th Hospital of Joint Logistics Support Force of Chinese People's Liberation Army, Kunming, Yunnan, China
[b] Department of Respiration, 920th Hospital of Joint Logistics Support Force of Chinese People's Liberation Army, Kunming, Yunnan, China
[c] Department of Plastic and Maxillofacial Surgery, The Second Affiliated Hospital of Chongqing Medical University, Chongqing, China
[d] Laboratory of Molecular Cardiology, Department of Cardiology, The First Affiliated Hospital of Kunming Medical University, Kunming, Yunnan, China

ARTICLE INFO

Keywords:
CEACAM1
Lymphangiogenesis
NSCLC
NF- kB

ABSTRACT

Background: Lung cancer causes significant mortality, with invasion and metastasis being the main features that cause most cancer deaths. Lymph node metastasis is the primary metastatic route in non-small cell carcinoma (NSCLC) and influences the staging and prognosis of NSCLC. Cumulative studies have reported that Carcinoembryonic antigen-related cell adhesion molecule 1 (CEACAM1) is involved in the progression of various cancers. However, few studies have discussed the function of CEACAM1 in lymphangiogenesis in NSCLC. Here, we examined how CEACAM1 influences lymphangiogenesis in NSCLC.

Methods: A total of 30 primary squamous cell carcinoma (LUSC) patients diagnosed with LN metastasis were prospectively selected. LUSC tumor tissues, para-cancerous tissues, and positive lymph node tissues were harvested. The expression and subcellular location of CEACAM1, CD31, and LVYE1 in clinical samples were detected by immunohistochemistry. Next, the CEACAM1 and hsa-miR-423-5p expressions were detected by qPCR. The protein expression of lymphangiogenesis-associated proteins and critical cytokines of the NF–κB pathway in HDLECs was detected by Western blot. A tube formation assay was performed to detect the lymphangiogenesis in different groups. The interaction between CEACAM1 and hsa-miR-423-5p was verified using a dual luciferase assay.

Results: CEACAM1 was found to be a potential gene associated with lung cancer prognosis. It was positively correlated with angiogenesis and lymphangiogenesis. Then, we detected the function of CEACAM1 in lymphangiogenesis and found that CEACAM1 promoted lymphangiogenesis. hsa-miR-423-5p overexpression inhibited lymphangiogenesis via targeting CEACAM1. Finally, we observed that CEACAM1 can activate the NF–κB pathway and, therefore, promote lymphangiogenesis.

Conclusion: We found that CEACAM1 enhanced lymphangiogenesis in NSCLC via NF-kB activation and was repressed by miR-423-5p. This suggests the value of CEACAM1 as a new therapeutic marker in NSCLC.

1. Introduction

Lung cancer, including small-cell carcinoma and non-small cell carcinoma (NSCLC), is the second most frequent cancer, following breast cancer in women and prostate cancer in men [1–3]. NSCLC is classified histologically into bronchial gland carcinoma (<5 %), carcinoid (<5 %), adenosquamous carcinoma (<5 %), large cell carcinoma (10 %), squamous cell carcinoma (LUSC, 25 %), and adenocarcinoma (LUAD, 40 %) [2,4,5]. The treatment of non-small cell lung cancer (NSCLC) represents a significant challenge for clinicians, given the disease's more aggressive nature compared to small cell lung cancer (SCLC) and the generally poor prognosis for patients with NSCLC [6]. Approximately 57 % of NSCLCs are diagnosed at an advanced stage, with corresponding 1-year and 5-year survival rates of 26 % and 4 %, respectively [5]. Invasion and metastasis of lung cancer into vital organs such as the liver, bone, and nervous system contribute to significant mortality [7,8]. It is estimated

* Corresponding author.
** Corresponding author.
E-mail addresses: zhaofeipengsc@163.com (F. Zhao), wangyan@ydyy.cn (Y. Wang).
[1] Authors contributed equally to this work.

https://doi.org/10.1016/j.bbrep.2024.101833
Received 1 July 2024; Received in revised form 15 September 2024; Accepted 19 September 2024

that the majority of deaths in stage III occur as a result of metastatic recurrence following surgical resection, and approximately 80 % of NSCLC patients are diagnosed after lymph node metastasis or distant organ metastasis [5,9,10]. Tumors with similar histopathology appear to differ at the molecular level, and these differences can be used to target therapies to different tumor types [11]. Therefore, it is important to understand the molecular mechanism in lung cancer.

Blood vessels and lymphatic vessels are two significant components in tumor metastasis [12,13]. Lymph node metastasis stands out as the foremost route of metastasis in NSCLC, significantly influencing its staging and prognosis [14,15]. The lymphatic system comprises circulating lymphocytes, lymphatic vessels, lymph nodes, and lymphatic organs [16,17]. Lymphatic vessels are characterized as thin-walled, low-pressure vessels with less dense cytoplasm of endothelial cells and discontinuous basement membrane. The antigen-presenting cells, lymphocytes, proteins, and intercellular fluid are transported to the circulation system and lymph nodes via the lymphatic vessels [18,19]. Lymphangiogenesis, the generation of new lymphatic vessels [20,21], is a crucial process linked to tumor metastasis and a negative prognosis in various epithelial cancers. Lymphangiogenesis is involved in colon cancer progression [22,23]. Kadota et al. [24] proved that lymphangiogenesis is independently associated with poor prognoses in NSCLC patients. Therefore, a treatment manipulating lymphangiogenesis will undoubtedly remain a novel and appealing strategy.

As a cell surface glycoprotein, carcinoembryonic antigen-related cell adhesion molecule 1 (CEACAM1) participates in intercellular binding [25,26]. CEACAMs have been found to exert insulin homeostasis [27], vascular neogenesis [28], and immune modulation [25]. CEACAM1 is found and induced not only on different epithelial cells but also various leukocytes [29]. Accumulated research has reported that CEACAM1 participates in the development of many cancers [30]. Nerbil et al. [29] showed that CEACAM1 could promote tumor lymphangiogenesis and induce the generation of lymphatic endothelial cells from vascular endothelial cells by targeting Prox1 and VEGFR-3. Also, Zhou et al. [31] proved that CEACAM1 promoted lymphangiogenesis and angiogenesis in oral carcinoma. However, little research discussed the function of CEACAM1 on lymphangiogenesis in NSCLC.

The present study identified CEACAM1 as a potential gene associated with lung cancer prognosis. A positive correlation was observed between the expression of the gene and the processes of angiogenesis and lymphangiogenesis. Subsequently, the function of CEACAM1 in lymphangiogenesis was investigated, and it was observed that CEACAM1 promoted lymphangiogenesis. Conversely, overexpression of hsa-miR-423-5p inhibited lymphangiogenesis by targeting CEACAM1. Additionally, it was demonstrated that CEACAM1 activates the NF-κB pathway, thereby promoting lymphangiogenesis. Based on these findings, CEACAM1 can be considered a potential target for clinical application (Supplement Fig. 1).

2. Materials and methods

2.1. Clinical tissues and tissue microarray construction

Thirty primary LUSC patients with LN metastasis were prospectively selected. LUSC tumor tissues, para-cancerous tissues, and positive lymph node tissues were harvested from the 920th Hospital of Joint Logistics Support Force of the Chinese People's Liberation Army between 2017 and 2019. All patients with primary LUSC received total resection. However, they did not receive chemotherapy or neoadjuvant radiotherapy. Histological diagnosis [32] and staging [33] were performed following the 2004 World Health Organization guidelines [34]. Tumor-node-metastasis (TNM) classification [35,36] was performed following the guidelines in the 8th edition of the AJCC/UICC TNM classification for lung cancer. Before specimen collection, all patients were provided with comprehensive information regarding the procedures and data retrieval methods and signed the informed consent. This study does not disclose any information that could disclose the identity of patients or infringe upon individual rights. The human protocols were implemented strictly on the basis of the Ethical Guidelines of the Declaration of Helsinki and was proven by the ethics committee of First People's Hospital of Yunnan Province (certification no. 2020-013-01).

Tissue microarray was constructed utilizing archival formalin-fixed, paraffin-embedded tissue blocks as described before [37,38]. Briefly, tissue microarray blocks were cut into serial sections (5 μm), which were then dissociated in xylene and rehydrated by grading the alcohol series into distilled water. Hematoxylin and eosin staining (Supplementary Fig. 2) was subsequently used to select representative pathological areas.

2.2. Immunohistochemistry and scores

We conducted immunohistochemistry as previous description [38,39]. The paraffin section was subjected to deparaffinization, rehydration, and heat-mediated antigen retrieval. After cooled down, sections were incubated with a pre-immune serum to block non-specific staining, followed by inactivation of endogenous peroxidase with methanol containing 0.3 % H_2O_2. Primary antibodies against CEACAM1 (isotype: IgG, 1:50, ab108397, Abcam, UK), CD31 (isotype: IgG, 1:50, ab28364, Abcam, UK), and Lymphatic endothelium hyaluronate receptor (LVYE1) (isotype: IgG, 1:2000, ab28364, Abcam, UK) were applied to the sections. Following rinsing with PBS, the samples were probed with the EnVisionTM + Dual Link System-HRP secondary antibody (Dako North America, Inc. Carpinteria, CA, USA) for 30 min at 37 °C. Color development was conducted with a chromogen solution and DAB (3, 3-diaminobenzidine). Counterstaining was performed using hematoxylin. A matched IgG isotype antibody was used as a negative control to determine the antibody specificity. The sections were examined utilizing the LSM710 laser scanning confocal microscopy (Carl Zeiss, Germany).

The immunohistochemistry staining score was determined by evaluating both the intensity and extent of the positive staining [38]. For staining intensity, negative staining was scored 0 points, weak staining (light brown) was scored 1 point, moderate staining (brown) was scored 2 points, and strong staining (dark brown) was scored 3 points. For the positive staining ratio, 0 % was scored 0 points, 1%–25 % was scored 1 point, 25%–50 % was scored 2 points, 50%–75 % was scored 3 points, and 75%–100 % was scored 4 points. The product of the ratio and intensity scores determined the final staining scores. Cut-off values were established considering the prognostic significance and distribution of the value. An agreement of 95 % was reached between the two evaluators, with any discrepancies being resolved by discussion.

2.3. Cell culture and transfection

BeNa Culture Collection (BNCC, Beijing, China) provided the human NSCLC cancer cell lines 95-D, A549, and PC-9 as well as the human bronchial epithelial cell line (BEAS-2B). The American Type Culture Collection (Manassas, VA, USA) provide the human NSCLC cancer cell lines A427 and HCC827. XWLC-05 was obtained from The Institute of Oncology of Yunnan Provincial Tumor Hospital. Cells were kept at 37 °C with 5 % CO_2 in RPMI 1640 (Hyclone, USA). The 1 % Penicillin/Streptomycin and 10 % fetal bovine serum (FBS) (Hangzhou Sijiqing Biotech, Co. Ltd. China) were added to the medium. GenePharma (Shanghai, China) synthesized the miR-423-5p mimic, miR-423-5p inhibitor, and the negative controls. GenePharma also provided the CEACAM1 expression plasmid pcDNA-CEACAM1, si-CEACAM1, and the negative controls. The plasmids were transfected to 95-D utilizing Lipofectamine 2000 (Invitrogen, Carlsbad, CA, USA). The transfection lasted for 48 h.

2.4. qPCR

Total RNA was isolated from cells utilizing the TRIzol reagent

(Invitrogen). The cDNA was generated utilizing the First Strand cDNA Synthesis Kit (Thermo Fisher Scientific, USA), followed by qPCR employing TB Green® Fast qPCR Mix (TaKaRa, Dalian, China). The 2-ΔΔCt method determined the relative levels. The internal control was U6. The primers included:

miR-423-5p forward: 5′-CGAAGTTCCCTTTGTCATCCT-3′
miR-423-5p reverse: 5′-GTGCAGGGTCCGAGGTATTC-3.
U6 forward: 5′-CTCGCTTCGGCAGCACA-3’;
U6 reverse 5′-AACGCTTCACGAATTTGCGT-3’.

2.5. Wound stretch assay

Wound stretch assay assessed cell migration [40]. Briefly, in a 6-well plate, cell seeding was conducted at a density of 5×10^5 to 1×10^6 cells/well. The cells were maintained in DMEM medium without FBS at 37 °C. Until the cells were grown to 80%–90 % confluent, the monolayer was made a scratch utilizing a pipette tip and the detached cells were removed. After 24 h, the width of the scratch was analyzed by ImageJ (version 1.80, National Institutes of Health, Bethesda, MD, USA). The migration index was determined using the formula: Migration index (%) = [(initial width of the scratch) - (final width of the scratch)]/(initial width of the scratch).

2.6. Western blot

Cellular proteins were obtained. The Bicinchoninic Acid Protein Assay Kit (KeyGen Biotech, China) measured their concentration. The proteins were then separated and transferred onto PVDF membranes, followed by blocking with 5 % skimmed milk for 2 h. Subsequent steps included primary antibody incubation (Table 1) at 4 °C, TBS-T rinsing, exposure to secondary antibodies, the application of enhanced chemiluminescence for color development, and intensity determination utilizing NIH Image J software.

2.7. Tube formation and immunofluorescence

Human dermal lymphatic endothelial cells (HDLEC, PromoCell, Germany, 1.5×10^4/well) were co-cultured with the A427 and highest in 95-D cell lines (7.5×10^3/well) and inoculated on 96-well plates previously coated with Matrigel membrane/matrix (BD, USA). After 6 h of incubation, micro-lymphatic vessels were observed, and the number of tubes was calculated [41].

After fixation in 4 % paraformaldehyde, the cells were probed for 2 h with primary antibody against CEACAM1 (isotype: IgG, 1:50, absin, China), followed by Alexa Fluor® 594-conjugated goat anti-rabbit IgG (Abcam, USA) incubation. DAPI stained the cell nuclei. Fluorescence images were observed and the mean intensity of fluorescence was analyzed using NIH Image J software.

Table 1
Primary antibodies used in Western blot.

Primary	Company	Catalog number	Dilution	Molecular weight	Species
CEACAM1	abcam	ab108397	1:10000	58	Rabbit
VEGF-C	abcam	ab83905	1:1000	46	Rabbit
VEGF-D	abcam	ab103685	1:1000	40	Rabbit
VEGFR3	abcam	Ab243232	1:1000	146	Rabbit
P65 NF-kB	abcam	ab32536	1:1000	65	Rabbit
p-P65 NF-kB	abcam	ab76302	1:1000	65	Rabbit
P50 NF-kB	abcam	ab32360	1:1000	44	Rabbit
P-p50	abcam	ab209765	1:1000	105	Rabbit
GAPDH	abmart	P30008 M	1:1000	37	Rabbit

2.8. Dual luciferase assay

The wild type and mutate type sequences of CEACAMA1 were cloned into the pGL3 vector (Promega, WI, USA). The plasmids, negative control oligonucleotides, and miR-146a-5p mimic (GenePharma) were co-transfected into 293T cells. After transfection for 48 h, we quantified the luciferase activity by utilizing the Dual-Luciferase Reporter Assay System (Promega, WI, USA).

2.9. Statistical analysis

Data analysis was carried out uitilizing SPSS version 20.0 (SPSS, Chicago, IL, USA). The Kolmogorov-Smirnov test assessed data distribution. Continuous data of normal distribution are presented as mean ± standard deviation (SD). One-way ANOVA and Tukey’s test were applied for multi-comparison. The Pearson correlation coefficient and chi-square test were used to assess the association of clinicopathological factors with CEACAM1, CD31, or LVYE1 expression in tumor, and positive lymph node tissues. $P < 0.05$ was deemed significant.

3. Results

3.1. CEACAM1 was positively expressed in tissues and exihited positive correlation with lymph node metastasis

First, the subcellular distribution and expression of CEACAM1 in clinical samples from primary LUSC patients diagnosed with lymph node metastasis were detected by immunohistochemistry. The baseline data are displayed in Supplement Table 1. According to the results, CEACAM1 was expressed in the cytoplasm and membrane. Also, CEACAM1 was positively expressed in tumor tissues and positive lymph nodes but low-positively expressed in corresponding para-cancerous tissues. Also, the area of positive CEACAM1 expression significantly increased in tumor and positive lymph nodes than in corresponding para-cancerous tissues (Fig. 1). Then, the expression of CEACAM1 in pan-cancer was predicted by TIMER (ver. 2.0). The analysis showed differential expression of CEACAM1 in 19 out of 24 cancer types (Supplementary Fig. 3A, Supplementary Table 2), which is higher expressed both in LUAD ($P < 0.001$) and LUSC ($P = 0.0102$). The KMplot [42] and the PrognoScan database [43] were used to evaluate the association of CEACAM1 mRNA with prognosis in LUAD and LUSC. There was a significant correlation between high CEACAM1 expression and poor prognosis in LUAD cohorts, while the correlation was not significant in LUSC cohorts (Supplementary Figs. 3B–E).

To further investigate the correlation of CEACAM1 with blood and lymphatic vessels, the expression and subcellular location of CD31, a regarded marker of vascular endothelial cell [44], and LVYE1, a regarded marker of the lymphatic vessel [12], was also detected. CD31 expression was found in the membrane and cytoplasm, while LVYE1 was found in the nucleus, membrane, and cytoplasm. CD31 and LVYE1 were low-positively expressed in tumor and positive lymph nodes while negatively expressed in para-cancerous tissues. The positive expression area of CD31 and LVYE1 was significantly elevated in corresponding para-cancerous tissues (Fig. 1). Based on the final staining scores, the relationship between clinicopathological status and CEACAM1, CD31, or LVYE1 expression in tumor and positive lymph node tissues. The CEACAM1 expression in tumor tissues was associated with the pathological stage (Table 2). Also, the correlation of CEACAM1 with CD31 or LVYE1 expression was analyzed using the Pearson chi-square test. It is observed that, CEACAM1 expression was positively correlated CD31 and LYVE1 in both tumor tissues (CD31 vs. CEACAM1: $P = 0.0113$, $r = 0.4559$; LYVE1 vs. CEACAM1: $P = 0.0029$, $r = 0.5243$) and positive lymph node (CD31 vs. CEACAM1: $P = 0.0117$, $r = 0.4541$; LYVE1 vs. CEACAM1: $P = 0.0008$, $r = 0.5778$) (Table 3). Which indicated that CEACAM1 was positively correlated with angiogenesis and lymphangiogenesis.

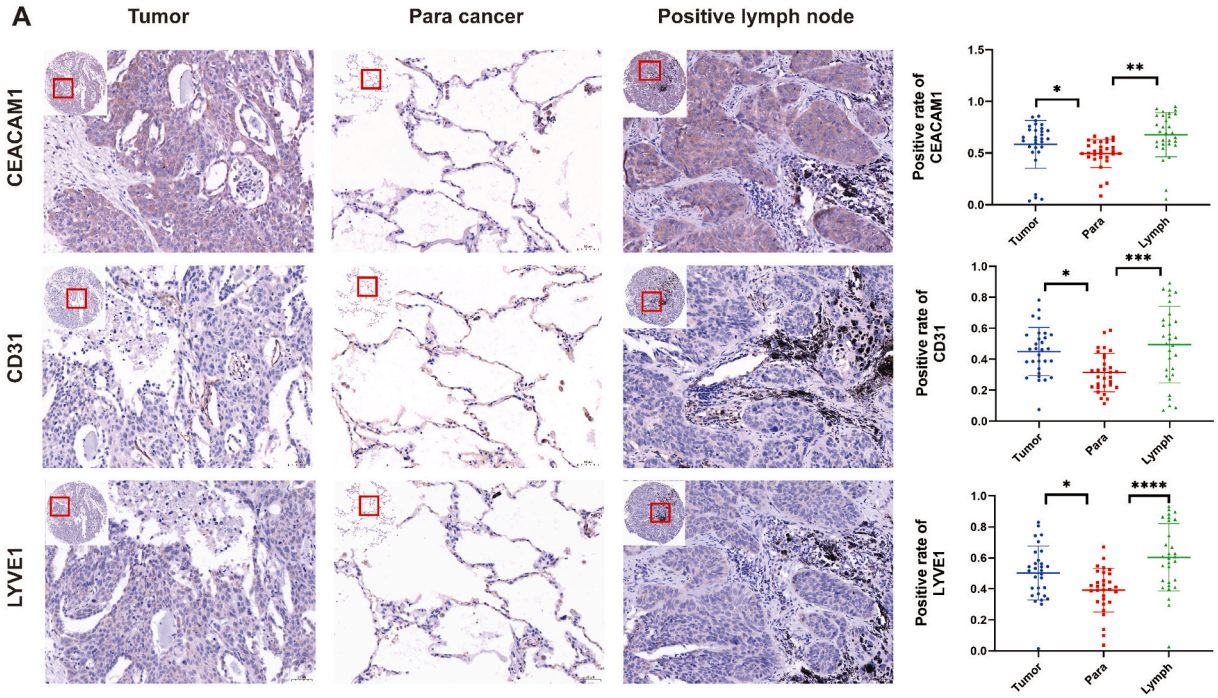

Fig. 1. CEACAM1 is positively expressed in LUSC tumor tissues and positive lymph node tissues. Immunohistochemistry staining and percentage of the positive area of CEACAM1, CD31, and LYVE1 in 30 LUSC tumor tissues and their corresponding para-cancerous tissues and positive lymph node tissues (*40, with *5 in the left corner). Error bars represent SD. *, $p < 0.05$; **, $p < 0.01$; ***, $p < 0.001$; ****, $p < 0.0001$.

3.2. CEACAM1 promoted lymphangiogenesis

Next, six NSCLC cell lines were selected, and a wound-healing assay was conducted to select the high- and low-metastatic cell lines. The results showed that 95-D exhibited a higher migration index than the other cell lines, while A427 exhibited the lowest (Fig. 2A). Also, the mRNA and protein expression of CEACAM1 was detected, and the expression was lowest in A427 and highest in 95-D (Fig. 2B and C). Therefore, A427 was defined as a low metastatic cell line, and 95-D was defined as a highly metastatic cell line for subsequent experiments. Then, si-NC and si-CEACAM1 were transfected into 95-D, and CEACAM1 was evaluated by Western blot (Fig. 2D). The protein expression of CEACAM1 in 95-D was higher than that in A427, while the transfection of si-CEACAM1 deprived the expression. Then, to detect the function of CEACAM1, NSCLC cell lines were co-cultured with HDLEC, and a tube formation assay was conducted. The protein expression of lymphangiogenesis-associated proteins in HDLEC, i.e., VEGFR3, VEGFC, and VEGFD, was also detected. The expression of VEGFR3, VEGFC, and VEGFD was higher in 95-D compared to A427, while the downregulation of CEACAM1 reduced the lymphangiogenesis-associated proteins (Fig. 2E) and suppressed tube formation (Fig. 2F). These results suggested that CEACAM1 potentially promoted lymphangiogenesis.

3.3. CEACAM1 was a target of hsa-miR-423-5p

Next, we predicted the miRNAs that target CEACMA1 by ENCORI [36], and hsa-miR-423-5p was selected as the supposed target due to putative binding region between the seed sequence of hsa-miR-423-5p and the 3′-UTR of CEACAM1 (Fig. 3A). The relative luciferase activity in the 293T cell line transfected with luciferase reporters containing the wild-type CEACAM1 was suppressed upon hsa-miR-423-5p up-regulation. However, no significant decrease was observed after transfection with mutant CEACAM1 (Fig. 3B). Also, the hsa-miR-423-5p was detected with qPCR, which revealed that the hsa-miR-423-5p level was lower in A427 than in Beas-2B and further lower in 95-D (Fig. 3C). Next, TCGA data also predicted that hsa-miR-423-5p expression was lower in tumor tissues than in normal lung tissue (Fig. 3D), which was coincident with the result in vitro. To evaluate the regulation of CEACAM1 by hsa-miR-423-5p, plasmids were transfected into 95-D. Western blot revealed that CEACAM1 expression was decreased after the upregulation of hsa-miR-423-5p, whereas when the hsa-miR-423-5p inhibitor was transfected, CEACAM1 expresion was increased (Fig. 3E). Therefore, hsa-miR-423-5p may target CEACAM1 and can negatively regulate the expression of CEACAM1.

3.4. Aberrant overexpression of hsa-miR-423-5p suppressed lymphangiogenesis via targeting CEACAM1

To examine the regulatory role of hsa-miR-423-5p in lymphangiogenesis through targeting CEACAM1, 95-D cells were transfected with plasmids designed to modulate the hsa-miR-423-5p and CEACAM1 expressions. The transfection effectiveness was validated through qPCR and Western blot analyses (Fig. 4A and B). The hsa-miR-423-5p mimics increased hsa-miR-423-5p expression while decreasing CEACAM1 expression. This decrease was reversed by subsequent transfection with the pcDNA-CEACAM1. These results indicated the successful transfection of plasmids. After co-culturing, the protein expression of lymphangiogenesis-associated proteins. i.e., VEGFR3, VEGFC, and VEGFD in HDLECs were decreased in HDLECs when hsa-miR-423-5p was upregulated in 95-D, while the increase of CEACAM1 expression reversed the result (Fig. 4C). Similarly, the tube formation was suppressed when hsa-miR-423-5p was overexpressed in 95-D, while the CEACAM1 overexpression reversed the suppression (Fig. 4D). Therefore, the hsa-miR-423-5p overexpression suppressed lymphangiogenesis via targeting CEACAM1.

3.5. CEACAM1 regulated the lymphangiogenesis via activating the NF–κB pathway

Then, we examined whether CEACAM1 can regulate the NF–κB pathway and therefore regulate lymphangiogenesis. First, the levels of key cytokines in the NF–κB pathway in HDLEC were analyzed with the

Table 2
Clinicopathological parameters of patients with CEACAM1, CD31and LYVE1 expression.

Category	No. of case	Expression															
		Tumor									Positive lymph node						
		CEACAM1			CD31			LYVE1			CEACAM1			CD31			LYVE1		
		Low, n (%)	High, n (%)	*P*	Low, n (%)	High, n (%)	*P*	Low, n (%)	High, n (%)	*P*	Low, n (%)	High, n (%)	*P*	Low, n (%)	High, n (%)	*P*	Low, n (%)	High, n (%)	*P*
Total	30, (100 %)	20, (66.67 %)	10, (33.33 %)		29, (96.67 %)	1, (3.33 %)		28, (93.33 %)	2, (6.67 %)		14, (46.67 %)	16, (53.33 %)		22, (73.33 %)	8, (26.67 %)		22, (73.33 %)	8, (26.67 %)	
Gender				0.942			0.658			0.658			0.485			0.179			0.244
Male	27, (90.00 %)	18, (66.67 %)	9, (33.33 %)		26, (96.30 %)	1, (3.70 %)		25, (92.59 %)	2, (7.41 %)		12, (44.44 %)	15, (55.56 %)		19, (70.37 %)	8, (29.63 %)		19, (70.37 %)	8, (29.63 %)	
Female	3, (10.00 %)	2, (66.67 %)	1, (33.33 %)		3, (100 %)	0, (0 %)		3, (100 %)	0, (0 %)		2, (66.67 %)	1, (33.33 %)		3, (100 %)	0, (0 %)		3, (100 %)	0, (0 %)	
Age				0.434			0.362			0.362			0.832			0.259			0.728
≥60	15, (50.00 %)	8, (53.33 %)	7, (46.67 %)		14, (93.33 %)	1, (6.67 %)		13, (85.67 %)	2, (13.33 %)		6, (40.00 %)	9, (60.00 %)		11, (73.33 %)	4, (28.57 %)		10, (66.67 %)	5, (33.33 %)	
<60	15, (50.00 %)	12, (80.00 %)	3, (20.00 %)		15, (100 %)	0, (0 %)		15, (100 %)	0, (0 %)		8, (53.33 %)	7, (46.67 %)		11, (73.33 %)	4, (25.00 %)		12, (80.00 %)	3, (20.00 %)	
Stage				**0.044**			0.362			0.728			0.176			0.295			0.527
I-II	28, (93.33 %)	20, (100 %)	8, (28.57 %)		27, (96.43 %)	1, (3.57 %)		26, (92.86 %)	2, (7.14 %)		14, (50.00 %)	14, (50.00 %)		20, (71.43 %)	8, (28.57 %)		21, (75.00 %)	7, (25.00 %)	
III-IV	2, (6.67 %)	0, (0 %)	2, (100 %)		2, (100 %)	0, (0 %)		2, (100 %)	0, (0 %)		0, (0 %)	2, (100 %)		2, (100 %)	0, (0 %)		1, (50.00 %)	1, (50.00 %)	
Tumor Position				0.653			0.728			0.244			0.104			0.146			0.280
Left lung lobe	18, (60.00 %)	12, (66.67 %)	6, (33.33 %)		18, (100 %)	0, (0 %)		17, (94.44 %)	1, (5.56 %)		7, (38.89 %)	11, (61.11 %)		11, (61.11 %)	7, (38.89 %)		11, (61.11 %)	7, (38.89 %)	
Right lung lobe	12, (40.00 %)	8, (66.67 %)	4, (33.33 %)		11, (91.67 %)	1, (8.33 %)		11, (91.67 %)	1, (8.33 %)		7, (58.33 %)	5, (41.67 %)		11, (91.67 %)	1, (8.33 %)		11, (61.11 %)	1, (8.33 %)	
N stage				0.803			0.391			0.850			0.962			0.236			0.709
N1	13, (43.33 %)	9, (69.23 %)	4, (30.77 %)		13, (100 %)	0, (0 %)		12, (92.31 %)	1, (7.69 %)		6, (46.15 %)	7, (53.85 %)		11, (84.62 %)	2, (15.38 %)		10, (76.92 %)	3, (23.08 %)	
N2	17, (56.67 %)	11, (64.71 %)	6, (35.29 %)		16, (94.12 %)	1, (5.88 %)		16, (94.12 %)	1, (5.88 %)		8, (47.06 %)	9, (52.94 %)		11, (64.71 %)	6, (35.29 %)		12, (70.59 %)	5, (29.41 %)	
Total number of lymph nodes				0.908			0.244			0.478			0.868			0.263			0.808
≥17	18, (60.00 %)	12, (66.67 %)	6, (33.33 %)		17, (94.4 %)	1, (5.56 %)		17, (94.44 %)	1, (5.56 %)		8, (44.44 %)	10, (55.56 %)		13, (72.22 %)	5, (27.78 %)		15, (83.33 %)	3, (16.67 %)	
<17	12, (40.00 %)	8, (66.67 %)	4, (33.33 %)		12, (100 %)	0, (0 %)		11, (91.67 %)	1, (8.33 %)		6, (50.00 %)	6, (50.00 %)		9, (75.00 %)	3, (25.00 %)		7, (52.33 %)	5, (41.67 %)	
Number of positive lymph nodes				0.236			0.478			0.685			0.626			0.942			0.879
≥3	18, (60.00 %)	13, (72.22 %)	5, (27.78 %)		17, (94.44 %)	1, (5.56 %)		17, (94.44 %)	1, (5.56 %)		8, (44.44 %)	10, (55.56 %)		13, (72.22 %)	5, (27.78 %)		13, (72.22 %)	5, (27.78 %)	
<3	12, (40.00 %)	7, (58.33 %)	5, (41.67 %)		12, (100 %)	0, (0 %)		11, (91.67 %)	1, (8.33 %)		6, (50.00 %)	6, (50.00 %		9, (75.00 %)	3, (25.00 %)		9, (75.00 %)	3, (25.00 %)	

Table 3
Association between CEACAM1 and CD31 or LYVE1 in NSCLC patients with LN metastasis.

CEACAM1 expression								
	Tumor				Positive lymph node			
	Low, n (%)	High, n (%)	Odds ratio (95 % CI)	*P*	Low, n (%)	High, n (%)	Odds ratio (95 % CI)	*P*
CD31			0.4559 (0.1145–0.7010)	**0.0113**			0.4541(0.1122–0.6999)	**0.0117**
High	9	1			10	6		
Low	20	0			12	2		
LYVE1			0.5243(0.2023–0.7440)	**0.0029**			0.5578(0.2747–0.7765)	**0.0008**
High	0	2			9	7		
Low	20	8			13	1		

Western blot. The ratio of P50, P65, and their phosphorylation was higher expressed in 95-D compared with A427. The hsa-miR-423-5p overexpression inhibited the ratio of P50 and P65, and their phosphorylation, and the overexpression of CEACAM1 reversed the results (Fig. 5).

To further verify the result, the 95-D transfected with si-CEACAM1 was treated with 10 nM BAY11-7085, a specific activator of NF–κB [45], and the effect of NF–κB pathway on lymphangiogenesis was observed. First, the expression of CEACAM1 and the ratio of P65 and its phosphorylation were detected (Fig. 6A–B), which revealed decreased expression of lymphangiogenesis-associated proteins in co-cultured HDLECs when the expression of CEACAM1 in 95-D was down-regulated. Interestingly, these effects were reversed by BAY11-7085 (Fig. 6C). Also, the stimulation of BAY11-7085 has no significant effect on CEACAM1 expression, but significantly increased the tube number of lymphatic vessels. These results proved that CEACAM1 can activate the NF–κB pathway and, therefore, promote lymphangiogenesis.

4. Discussion

Although remarkable advances have been made in understanding the risk, progress, and treatment options of lung cancer, its mortality remains high [46]. Distant metastasis of lung cancer is the main cause that induces an unfavorable prognosis, during which cancer cells secrete soluble mediators and spread to a distant organism through the bloodstream or lymphatic systems [47,48]. Here, our results observed that CEACAM1 was positively expressed in positive lymph nodes and tumor tissues from the LUSC patients who were diagnosed with lymph node metastasis. Moreover, CEACAM1 was found as a potential gene linked to lung cancer prognosis and positively correlated with angiogenesis and lymphangiogenesis. Then, we detected the function of CEACAM1 in lymphangiogenesis and found CEACAM1 promoted lymphangiogenesis through the NF–κB pathway, while the aberrant overexpressed of hsa-miR-423-5p suppressed the lymphangiogenesis by targeting CEACAM1.

The lymphatic vessels are essential and play a critical role in maintaining tissue fluid balance, transporting immune cells, and absorbing dietary fats [49]. In the early stage, the metastasis of lung cancer mainly depends on the lymphatic system [50]. Lymphangial capillaries are not encapsulated by smooth muscle cells or pericytes, and the ECM networks of the perineural lymphatic vessels are less dense than around the intratumoral vessels [51]. The lymphatic vessels' structure inevitably reduces the tumor invasion barrier and allows the entrance of ameboid and mesenchymal cells into the lymphatic circulation [52]. was positively correlated CD31 and LYVE1 in both tumor tissues is the growth process of lymphatic vessels, which occurs during inflammation, wound healing, and tumor metastasis [49]. Recent reports indicated that lymphangiogenesis involved pathological processes and was Closely associated with clinical prognosis in multiple cancers. Maria et al. [53] evidenced lymphangiogenesis-inducing vaccines elicit T cell immunity against melanomas and provide lymphangiogenesis induction as a potential immunotherapeutic strategy in melanoma treatment. Hwang [9] and Liu [54] proved that lymphangiogenesis could serve as a distinct prognostic indicator for NSCLC survival. The molecular mechanism of angiogenesis, the process of blood vessel growth, has been intensely discussed over the past few decades. Still, there is much more to be explored in the investigation of the molecular mechanisms of lymphangiogenesis. A significant obstacle to lymphangiogenesis research is up to the absence of specific monoclonal antibodies that selectively identify the lymphatic vascular endothelium [18]. Vascular endothelial growth (VEGF)-C and VEGF-D are prevalent and participate in lymphangiogenesis through enhancing the migration and growth of lymphatic endothelium cells [55]. Vascular endothelial growth factor receptor 3 (VEGF3R) belongs to the IIIrd class of tyrosine receptors [18] and is the primary receptor of lymphatic endothelium [56]. As a receptor of VEGF-C and VEGF-D, it is activated by its ligands, and tyrosine kinase in its intracellular domain stimulates the lymphatic endothelial cell proliferation [38]. Lymphatic endothelial hyaluronan receptor (LYVE-1), a hyaluronan receptor located in the endothelium of lymphatic vessels, has recently been implicated as a selective marker of lymphatic endothelium, presumably attributable to the critical role of the lymphatic system in hyaluronan metabolism [49]. It was found that, the expression of CEACAM1 was positively correlated CD31 and LYVE1 in both tumor tissues. This indicated the correlation of CEACAM1 in lymphangiogenesis. Also, when the expression of CEACAM1 decreased, the expression of VEGFC, VEGFD, and VEGFR3 was also decreased, so as the number of neoplastic lymphatic vessels, which proved the function of CEACAM1 in lymphangiogenesis in NSCLC.

Consistent with the notion in this manuscript, CEACAM1 is proven to correlate with the prognosis [37] and participates in including inflammation, angiogenesis, tumor progression, and metastasis [38]. Thus, it is considered a potential target of clinical treatment. An increase in CEACAM1 expression and CEACAM1-S/CEACAM1-L ratio promotes the progression of NSCLC [39]. In contrast, the restoration of CEACAM1 expression in some tumor lines has been found to abolish their oncogenicity. Therefore, CEACAM1 is considered a tumor suppressor [21], which reflects the intricate complexity of the role of CEACAM1 in cancer progression. CEACAM1 was upregulated in NSCLC cell lines, tumors, and positive lymph node tissues. Also, CEACAM1 exhibited a positive correlation with the CD31 and LVYE1 expression in both tumor and positive lymph node tissues, indicating that CEACAM1 was correlated with angiogenesis and lymphangiogenesis. Also, our results proved that CEACAM1 could promote the expression of lymphangiogenesis-associated proteins and, therefore, promote lymphangiogenesis in highly metastasis NSCLC cell lines. Also, we found that CEACAM1 promoted the activation of the NF–κB pathway, thereby regulating lymphangiogenesis. Prangsaengtong [57] et al. found that shikonin played an inhibitory role in lymphangiogenesis via negatively regulating the NF-κB/HIF-1α axis, which is consistent with our results.

MicroRNAs are non-coding RNAs that include approximately 22 nucleotides [58,59]. With considerable attention paid to their function in different biological processes over the past few decades, the deregulation of miRNA expression has been proven to be correlated with developmental defects and tumor progression [50,58]. Chen et al. [58] has proved that miRNA-148a was a prognostic factor for NSCL and

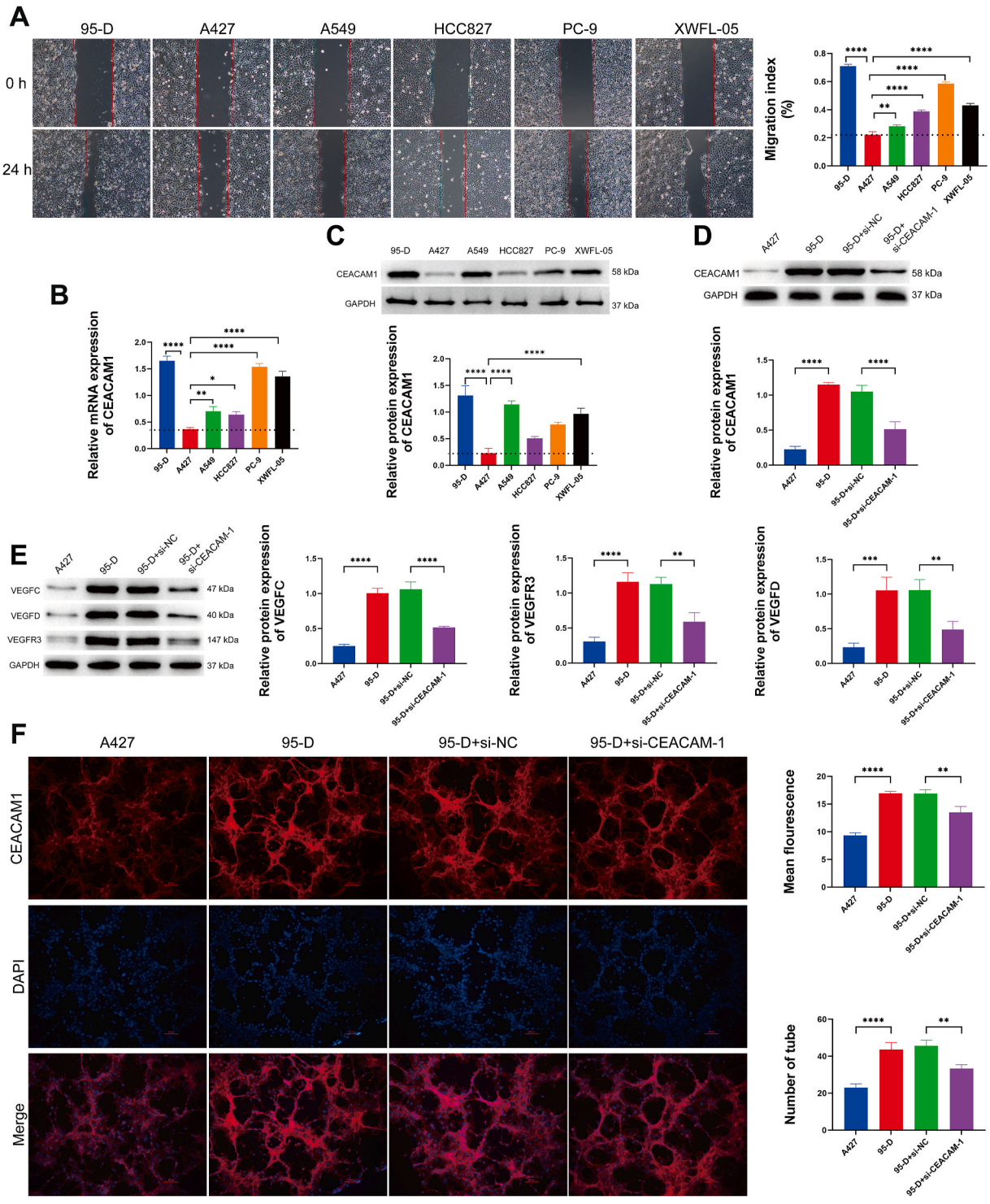

Fig. 2. CEACAM1 promoted the lymphangiogenesis. (A) NSCLC cell lines 95-D, A427, A549, HCC827, PC-9, and XWLC-05 were selected, and a wound healing assay was performed to select the highly and low metastatic cell lines (*10). The migration indexes were also calculated. (B) The mRNA expression of CEACAM1 in the NSCLC cell line was detected by qPCR. (C) The protein expression of CEACAM1 in the NSCLC cell line was detected by Western blot. (D) Western blot was used to verify the transfection efficiency. (E) The protein expression of lymphangiogenesis-associated proteins in HDLEC was detected by Western blot. (F) Tube formation assay was conducted, and Immunofluorescence detected the expression of CEACAM1. Error bars represent SD. *, $p < 0.05$; **, $p < 0.01$; ***, $p < 0.001$; ****, $p < 0.0001$.

inhibited its invasion and migration by Wnt1. The miRNA microarray analysis from Wu et al. suggested that miR-422a participated in lymphatic metastasis [60]. Meng et al. [61] also proved that microRNA-31 had potential as a predictive indicator for the survival and lymph node metastases in LUAD patients. We selected hsa-miR-423-5p as an upstream gene to target and regulate the CEACAM1. Several researchers have made progress on the function of hsa-miR-423-5p in cancers. Sun et al. [62] reported that breast cancer progression was suppressed by LINC00968 and the mechanism was through PROX1 inhibition medicated by hsa-miR-423-5p. Tian et al. [63] identified MYC

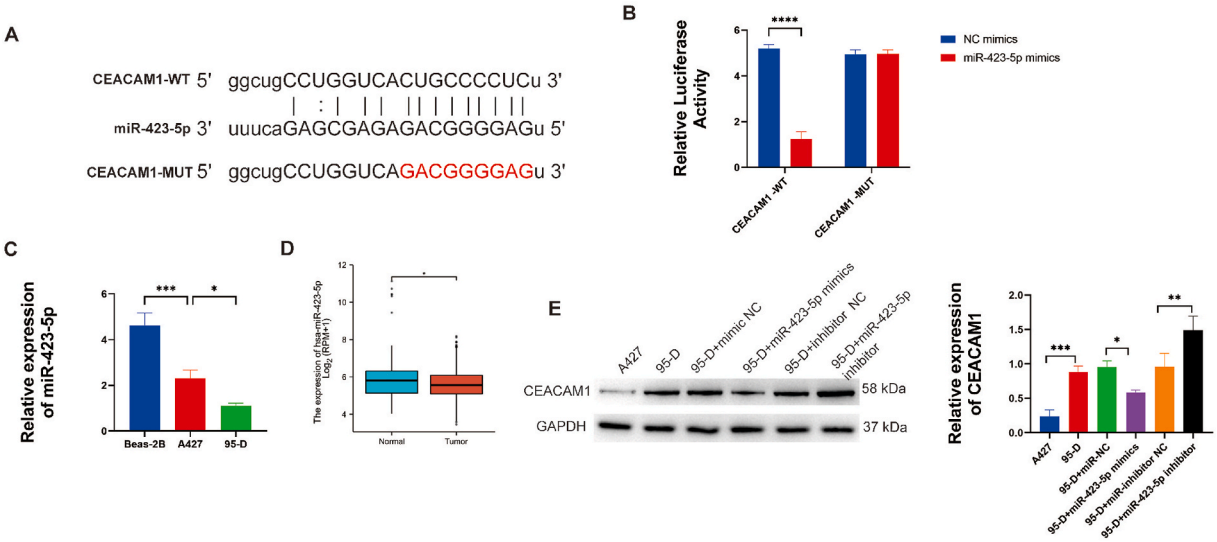

Fig. 3. CEACAM1 promoted the lymphangiogenesis. (A) Structure of human CEACAM1 gene and location of hsa-miR-423-5p. (B) Relative luciferase activity of different groups. (C) Relative expression of hsa-miR-423-5p was detected by qPCR. (D) TCGA data predicted the expression of hsa-miR-423-5p. (E) the protein expression of CEACAM1 regulated by hsa-miR-423-5p. Error bars represent SD. *, $p < 0.05$; **, $p < 0.01$; ***, $p < 0.001$; ****, $p < 0.0001$.

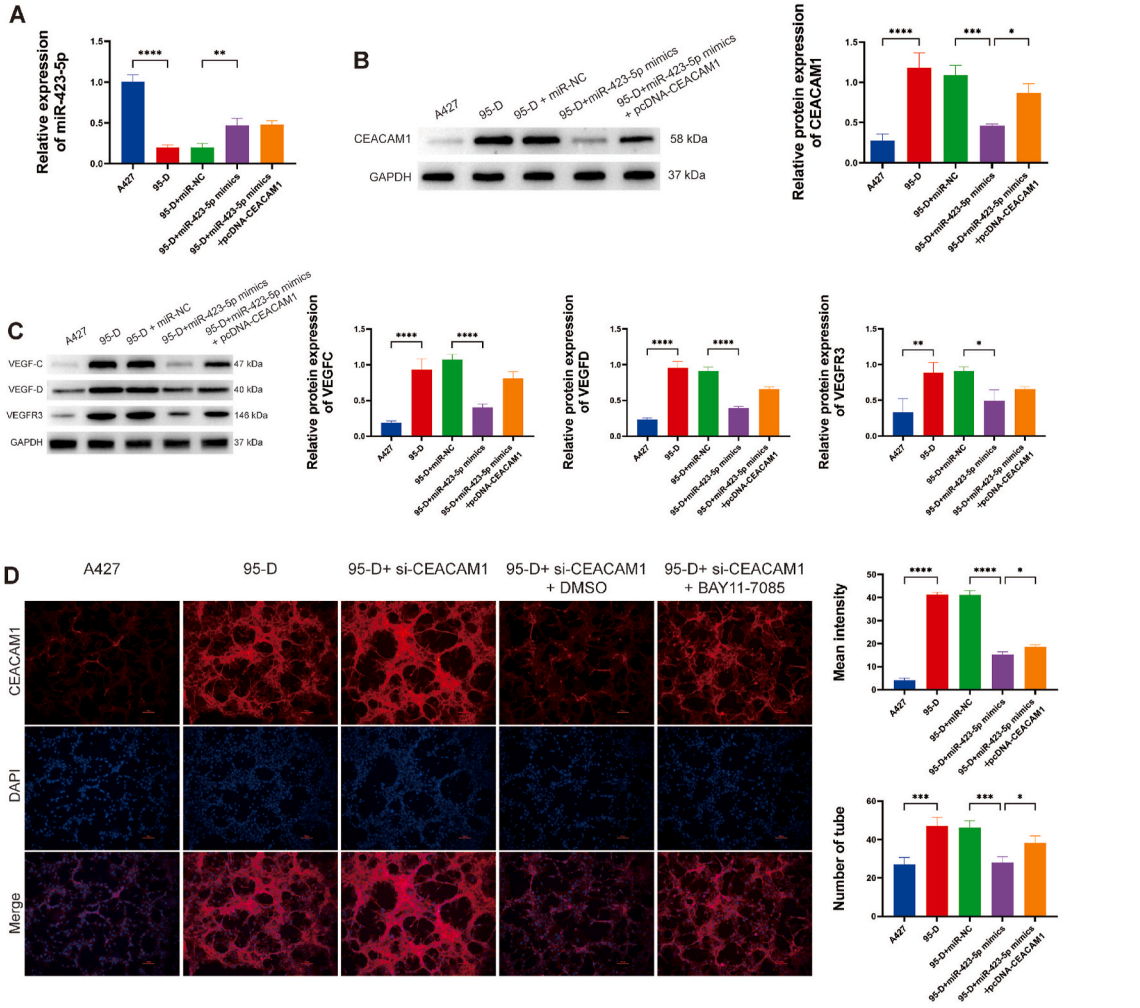

Fig. 4. Aberrant overexpression of hsa-miR-423-5p suppressed Lymphangiogenesis via targeting CEACAM1. (A) The relative expression of hsa-miR-423-5p was detected by qPCR after plasmid transfection. (B) The protein expression of CEACAM1 was detected by Western blot after plasmid transfection. (C) The protein expression of lymphangiogenesis-associated proteins in HDLEC was detected by Western blot. (D) Tube formation assay was conducted, and Immunofluorescence detected the expression of CEACAM1. Error bars represent SD. *, $p < 0.05$; **, $p < 0.01$; ***, $p < 0.001$; ****, $p < 0.0001$.

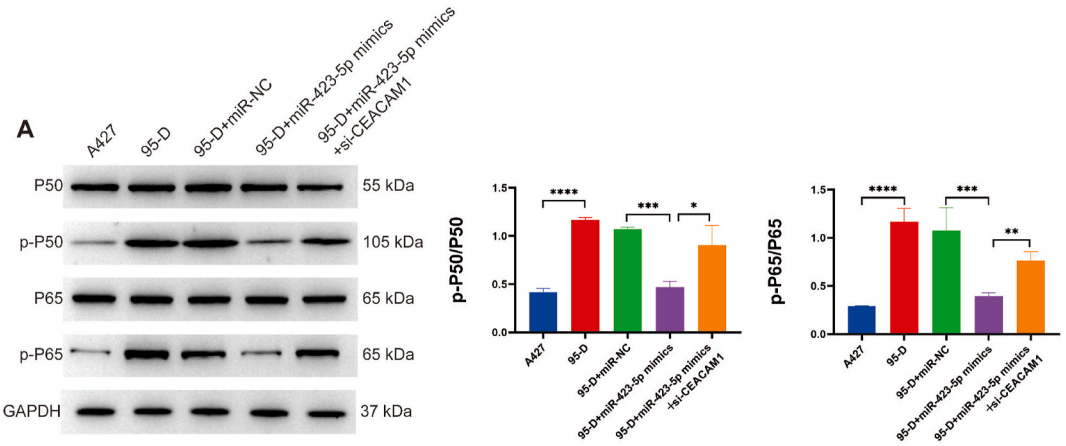

Fig. 5. CEACAM1 regulated the activation of the NF–κB pathway. (A) the protein expression of p50 and p65 and their phosphorylation were detected by Western blot. Error bars represent SD. *, $p < 0.05$; **, $p < 0.01$; ***, $p < 0.001$; ****, $p < 0.0001$.

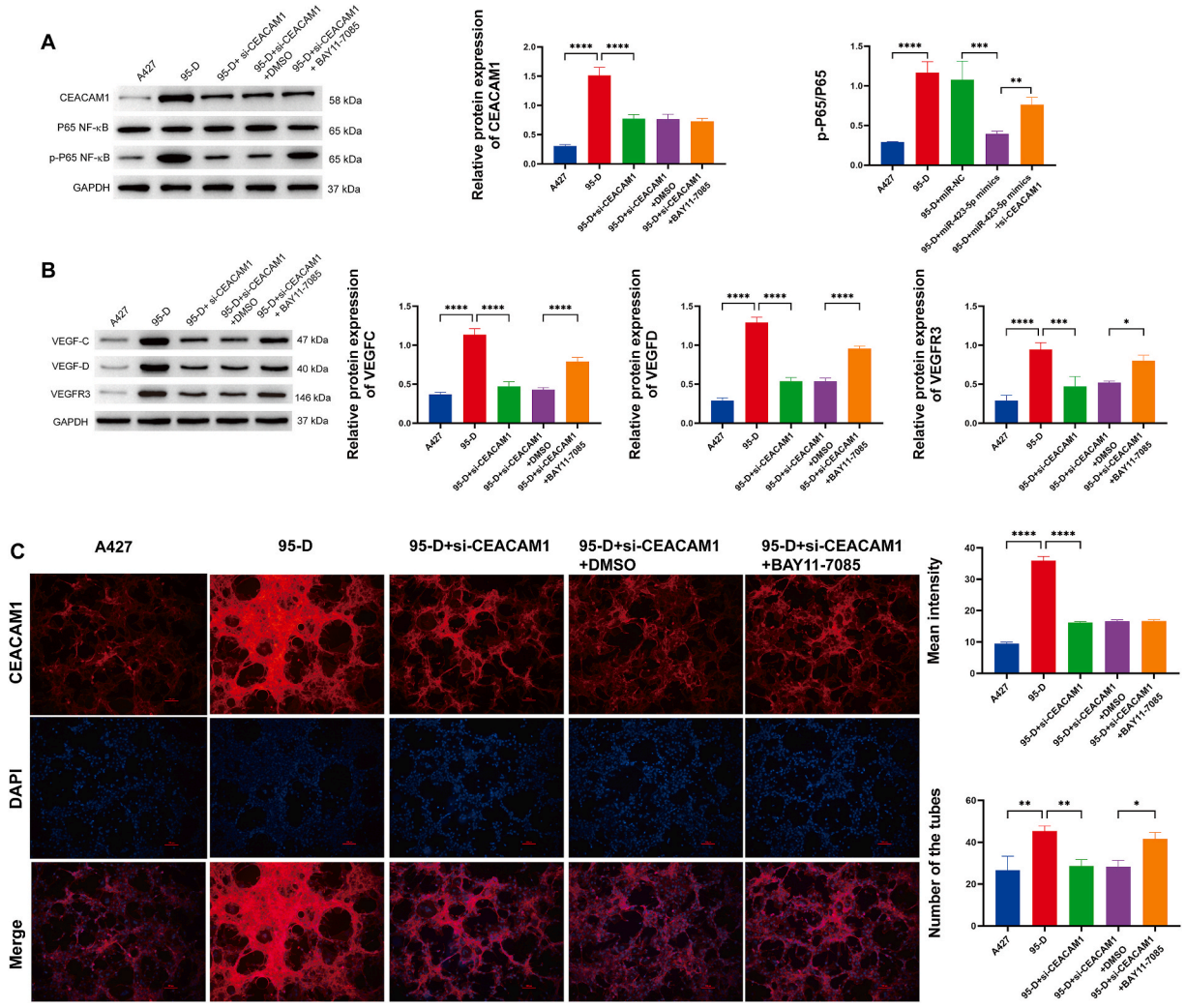

Fig. 6. CEACAM1 can activate the NF–κB pathway and promote lymphangiogenesis. (A) The expression of CEACAM1 and p65 and its phosphorylation was detected by Western blot. (B) The protein expression of lymphangiogenesis-associated proteins in HDLEC was detected by Western blot. (C) Tube formation assay was conducted, and Immunofluorescence detected the expression of CEACAM1. Error bars represent SD. *, $p < 0.05$; **, $p < 0.01$; ***, $p < 0.001$; ****, $p < 0.0001$.

and has-miR-423-5p as critical factors in nasopharyngeal carcinoma through miRNA-mRNA-pathway network analysis. Our results demonstrated that aberrant hsa-miR-423-5p overexpression suppressed lymphangiogenesis via targeting CEACAM1.

In conclusion, we found that CEACAM1 increased lymphangiogenesis through NF- kB pathway activation and inhibited miR-423-5p in

NSCLC. This indicated the value of CEACAM1 as a new therapeutic target targeting lymphangiogenesis in NSCLC. However, more researches, such as the role of CEACAM1 in lymphangiogenesis in primary lung cancer model, need further discussion. Also, the downstream of CEACAM1 should also discussed with the help of high-throughput detection to further understand the mechanism of CEACAM1 in lymphangiogenesis in NSCLC.

Ethics approval and consent to participate

Before specimen collection, all patients were provided with comprehensive information regarding the procedures and data retrieval methods and signed the informed consent. This study does not disclose any information that could disclose the identity of patients or infringe upon individual rights. The human protocols were implemented strictly on the basis of the Ethical Guidelines of the Declaration of Helsinki and was proven by the ethics committee of First People's Hospital of Yunnan Province (certification no. 2020-013-01).

Consent for publication

All data used during the study are available from the corresponding author by request.

Availability of data and material

All data generated or used during the study are available from the corresponding author by request.

Funding

This work was supported by 1) National Natural Science Foundation of China (82160076); 2) Young Talents of Yunnan Thousand Talents Plan (No. RLQB20220011); 3) 535 Talent Project of First Affiliated Hospital of Kunming Medical University (No. 2023535Q04); 4) Yunnan province science and technology department, Joint special fund project of Kunming Medical University applied basic research, general program (202101AY070001-303); 5) In-hospital Technology Program of 920th Hospital of Joint Logistics Support Force (2023ygy12).

CRediT authorship contribution statement

Jie Yu: Writing – original draft, Methodology, Funding acquisition, Formal analysis, Conceptualization. **Wenke Cai:** Writing – review & editing, Writing – original draft, Methodology, Investigation, Formal analysis. **Tao Zhou:** Writing – original draft, Formal analysis. **Bo Men:** Writing – review & editing, Methodology, Investigation, Formal analysis. **Shunqiong Chen:** Investigation, Formal analysis. **Dong Tu:** Writing – original draft, Visualization, Validation, Software, Methodology, Formal analysis, Conceptualization. **Wei Guo:** Writing – review & editing, Methodology, Investigation. **Jicui Wang:** Investigation. **Feipeng Zhao:** Writing – original draft, Software. **Yan Wang:** Writing – review & editing, Visualization, Validation, Supervision, Methodology, Funding acquisition, Conceptualization.

Declaration of competing interest

No benefits in any form have been or will be received from a commercial party related directly or indirectly to the subject of this manuscript.

Data availability

Data will be made available on request.

Acknowledgements

NONE.

Appendix A. Supplementary data

Supplementary data to this article can be found online at https://doi.org/10.1016/j.bbrep.2024.101833.

References

[1] A.G. Schwartz, M.L. Cote, Epidemiology of lung cancer, Adv. Exp. Med. Biol. 893 (2016) 21–41.
[2] L.G. Collins, et al., Lung cancer: diagnosis and management, Am. Fam. Physician 75 (1) (2007) 56–63.
[3] Y. Li, B. Yan, S. He, Advances and challenges in the treatment of lung cancer, Biomed. Pharmacother. 169 (2023) 115891.
[4] W.D. Travis, Pathology of lung cancer, Clin. Chest Med. 23 (1) (2002) 65–81, viii.
[5] P.C. Hoffman, A.M. Mauer, E.E. Vokes, Lung cancer, Lancet 355 (9202) (2000) 479–485.
[6] M. Entezari, et al., Long non-coding RNAs and exosomal lncRNAs: potential functions in lung cancer progression, drug resistance and tumor microenvironment remodeling, Biomed. Pharmacother. 150 (2022) 112963.
[7] J. Li, et al., Association between VEGFR-3 expression and lymph node metastasis in non-small-cell lung cancer, Exp. Ther. Med. 9 (2) (2015) 389–394.
[8] A.J. Abadi, et al., Small in size, but large in action: microRNAs as potential modulators of PTEN in breast and lung cancers, Biomolecules 11 (2) (2021).
[9] I. Hwang, et al., Tumor-associated macrophage, angiogenesis and lymphangiogenesis markers predict prognosis of non-small cell lung cancer patients, J. Transl. Med. 18 (1) (2020) 443.
[10] M. Ashrafizadeh, et al., Crosstalk of long non-coding RNAs and EMT: searching the missing pieces of an incomplete puzzle for lung cancer therapy, Curr. Cancer Drug Targets 21 (8) (2021) 640–665.
[11] M. Ashrafizadeh, et al., Therapeutic potential of AMPK signaling targeting in lung cancer: advances, challenges and future prospects, Life Sci. 278 (2021) 119649.
[12] Y.J. Lee, et al., Risk factors for lymph node metastasis in early colon cancer, Int. J. Colorectal Dis. 35 (8) (2020) 1607–1613.
[13] J.Y. Deng, H. Liang, Clinical significance of lymph node metastasis in gastric cancer, World J. Gastroenterol. 20 (14) (2014) 3967–3975.
[14] X. Xue, et al., Independent risk factors for lymph node metastasis in 2623 patients with Non-Small cell lung cancer, Surg Oncol 34 (2020) 256–260.
[15] R.U. Osarogiagbon, et al., The international association for the study of lung cancer lung cancer staging project: overview of challenges and opportunities in revising the nodal classification of lung cancer, J. Thorac. Oncol. 18 (4) (2023) 410–418.
[16] M.A. Swartz, The physiology of the lymphatic system, Adv. Drug Deliv. Rev. 50 (1–2) (2001) 3–20.
[17] Y. Li, et al., Lymphatic drainage system and lymphatic metastasis of cancer cells in the mouse esophagus, Dig. Dis. Sci. 68 (3) (2023) 803–812.
[18] B. Weryńska, P. Dziegiel, R. Jankowska, Role of lymphangiogenesis in lung cancer, Folia Histochem. Cytobiol. 47 (3) (2009) 333–342.
[19] G. Bertoldi, et al., Lymphatic vessels and the renin-angiotensin-system, Am. J. Physiol. Heart Circ. Physiol. 325 (4) (2023) H837–h855.
[20] M. Skobe, M. Detmar, Structure, function, and molecular control of the skin lymphatic system, J. Invest. Dermatol. Symp. Proc. 5 (1) (2000) 14–19.
[21] M.H. Witte, et al., Lymphangiogenesis and lymphangiodysplasia: from molecular to clinical lymphology, Microsc. Res. Tech. 55 (2) (2001) 122–145.
[22] M. Nagahashi, et al., Lymphangiogenesis: a new player in cancer progression, World J. Gastroenterol. 16 (32) (2010) 4003–4012.
[23] Q. Zhang, et al., ETV4 mediated tumor-associated neutrophil infiltration facilitates lymphangiogenesis and lymphatic metastasis of bladder cancer, Adv. Sci. 10 (11) (2023) e2205613.
[24] K. Kadota, et al., The clinical significance of lymphangiogenesis and angiogenesis in non-small cell lung cancer patients, Eur. J. Cancer 44 (7) (2008) 1057–1067.
[25] S.D. Gray-Owen, R.S. Blumberg, CEACAM1: contact-dependent control of immunity, Nat. Rev. Immunol. 6 (6) (2006) 433–446.
[26] H. Hirao, et al., Neutrophil CEACAM1 determines susceptibility to NETosis by regulating the S1PR2/S1PR3 axis in liver transplantation, J. Clin. Invest. 133 (3) (2023).
[27] A.M. DeAngelis, et al., Carcinoembryonic antigen-related cell adhesion molecule 1: a link between insulin and lipid metabolism, Diabetes 57 (9) (2008) 2296–2303.
[28] C. Wagener, S. Ergün, Angiogenic properties of the carcinoembryonic antigen-related cell adhesion molecule 1, Exp. Cell Res. 261 (1) (2000) 19–24.
[29] N. Kilic, et al., Lymphatic reprogramming of microvascular endothelial cells by CEA-related cell adhesion molecule-1 via interaction with VEGFR-3 and Prox1, Blood 110 (13) (2007) 4223–4233.
[30] V. Fiori, M. Magnani, M. Cianfriglia, The expression and modulation of CEACAM1 and tumor cell transformation, Ann. Ist. Super Sanita 48 (2) (2012) 161–171.
[31] C.J. Zhou, et al., CEACAM1 distribution and it's effects on angiogenesis and lymphangiogenesis in oral carcinoma, Oral Oncol. 45 (10) (2009) 883–886.
[32] A. Marx, et al., The 2015 World Health organization classification of tumors of the thymus: continuity and changes, J. Thorac. Oncol. 10 (10) (2015) 1383–1395.
[33] D.J. Boffa, F.L. Greene, Reacting to changes in staging designations in the 7th edition of the AJCC staging manual, Ann. Surg Oncol. 18 (1) (2011) 1–3.

[34] J. Fukuoka, et al., Chromatin remodeling factors and BRM/BRG1 expression as prognostic indicators in non-small cell lung cancer, Clin. Cancer Res. 10 (13) (2004) 4314–4324.
[35] P. Goldstraw, et al., The IASLC lung cancer staging project: proposals for revision of the TNM stage groupings in the forthcoming (eighth) edition of the TNM classification for lung cancer, J. Thorac. Oncol. 11 (1) (2016) 39–51.
[36] W. Lim, et al., The 8(th) lung cancer TNM classification and clinical staging system: review of the changes and clinical implications, Quant. Imag. Med. Surg. 8 (7) (2018) 709–718.
[37] Q. Wen, et al., CGP57380 enhances efficacy of RAD001 in non-small cell lung cancer through abrogating mTOR inhibition-induced phosphorylation of eIF4E and activating mitochondrial apoptotic pathway, Oncotarget 7 (19) (2016) 27787–27801.
[38] H. Kitano, et al., Synaptonemal complex protein 3 is associated with lymphangiogenesis in non-small cell lung cancer patients with lymph node metastasis, J. Transl. Med. 15 (1) (2017) 138.
[39] Q. Wen, et al., Flot-2 expression correlates with EGFR levels and poor prognosis in surgically resected non-small cell lung cancer, PLoS One 10 (7) (2015) e0132190.
[40] K. Chang, et al., lncRNA TTN-AS1 upregulates RUNX1 to enhance glioma progression via sponging miR-27b-3p, Oncol. Rep. 44 (3) (2020) 1064–1074.
[41] M. Iolyeva, et al., Novel role for ALCAM in lymphatic network formation and function, Faseb. J. 27 (3) (2013) 978–990.
[42] B. Győrffy, et al., Online survival analysis software to assess the prognostic value of biomarkers using transcriptomic data in non-small-cell lung cancer, PLoS One 8 (12) (2013) e82241.
[43] H. Mizuno, et al., PrognoScan: a new database for meta-analysis of the prognostic value of genes, BMC Med. Genom. 2 (2009) 18.
[44] F.M. Marelli-Berg, et al., An immunologist's guide to CD31 function in T-cells, J. Cell Sci. 126 (Pt 11) (2013) 2343–2352.
[45] J.W. Pierce, et al., Novel inhibitors of cytokine-induced IkappaBalpha phosphorylation and endothelial cell adhesion molecule expression show anti-inflammatory effects in vivo, J. Biol. Chem. 272 (34) (1997) 21096–21103.
[46] X. Wang, A.A. Adjei, Lung cancer and metastasis: new opportunities and challenges, Cancer Metastasis Rev. 34 (2) (2015) 169–171.
[47] L. Yin, et al., The role of exosomes in lung cancer metastasis and clinical applications: an updated review, J. Transl. Med. 19 (1) (2021) 312.
[48] I. Martinez-Espinosa, J.A. Serrato, B. Ortiz-Quintero, The role of exosome-derived microRNA on lung cancer metastasis progression, Biomolecules 13 (11) (2023).
[49] T. Tammela, K. Alitalo, Lymphangiogenesis: molecular mechanisms and future promise, Cell 140 (4) (2010) 460–476.
[50] F. Fazi, G. Fontemaggi, MicroRNAs and lymph node metastatic disease in lung cancer, Thorac. Surg. Clin. 22 (2) (2012) 167–175.
[51] S. Karaman, M. Detmar, Mechanisms of lymphatic metastasis, J. Clin. Invest. 124 (3) (2014) 922–928.
[52] K. Alitalo, The lymphatic vasculature in disease, Nat Med 17 (11) (2011) 1371–1380.
[53] M.S. Sasso, et al., Lymphangiogenesis-inducing vaccines elicit potent and long-lasting T cell immunity against melanomas, Sci. Adv. 7 (13) (2021).
[54] L. Liu, et al., Novel genetic variants of SYK and ITGA1 related lymphangiogenesis signaling pathway predict non-small cell lung cancer survival, Am. J. Cancer Res. 10 (8) (2020) 2603–2616.
[55] M.J. Karkkainen, K. Alitalo, Lymphatic endothelial regulation, lymphoedema, and lymph node metastasis, Semin. Cell Dev. Biol. 13 (1) (2002) 9–18.
[56] M.I. Koukourakis, et al., LYVE-1 immunohistochemical assessment of lymphangiogenesis in endometrial and lung cancer, J. Clin. Pathol. 58 (2) (2005) 202–206.
[57] O. Prangsaengtong, et al., Shikonin suppresses lymphangiogenesis via NF-κB/HIF-1α Axis inhibition, Biol. Pharm. Bull. 41 (11) (2018) 1659–1666.
[58] Y. Chen, et al., miRNA-148a serves as a prognostic factor and suppresses migration and invasion through Wnt1 in non-small cell lung cancer, PLoS One 12 (2) (2017) e0171751.
[59] H. Yang, et al., MiRNA-based therapies for lung cancer: opportunities and challenges? Biomolecules 13 (6) (2023).
[60] L. Wu, et al., Circulating microRNA-422a is associated with lymphatic metastasis in lung cancer, Oncotarget 8 (26) (2017) 42173–42188.
[61] W. Meng, et al., MicroRNA-31 predicts the presence of lymph node metastases and survival in patients with lung adenocarcinoma, Clin. Cancer Res. 19 (19) (2013) 5423–5433.
[62] X. Sun, et al., Long non-coding RNA LINC00968 reduces cell proliferation and migration and angiogenesis in breast cancer through up-regulation of PROX1 by reducing hsa-miR-423-5p, Cell Cycle 18 (16) (2019) 1908–1924.
[63] H. Tian, et al., MYC and hsa-miRNA-423-5p as biomarkers in nasopharyngeal carcinoma revealed by miRNA-mRNA-pathway network integrated analysis, Mol. Med. Rep. 16 (2) (2017) 1039–1046.